Nigerian Journal of Physics (NJP)
ISSN online: 3027-0936
ISSN print: 1595-0611
DOI: https://doi.org/10.62292/njp.v35(S).2026.544
Volume 35(S), 2026

Phase-Dependent Electronic Band Structure and Thermal Conductivity in Monolayer CrI_3 : *ab Initio* Insights for Spintronic Device Applications

[*1]Musa Muhammad Elbulatory, [2]Ibrahim Maijawa, [3]Abdullahi Muhammad Gidado, [4]Suleiman Ahmed Manjo

[1]Department of Physics, Yobe State University, Damaturu, Yobe State, Nigeria.
[2]Department of Physics, Federal University Gashua, Yobe State, Nigeria.
[3]Department of Physics, Federal University Birnin Kebbi, Kebbi State, Nigeria.
[4]Department of Physics, Federal University Dutse, Jigawa State, Nigeria.

*Corresponding Author's Email: MMElbulatory@ysu.edu.ng Phone: +2348032439496

Keywords:
2D Materials,
Ab Initio DFT Calculations,
Magnetic Phase-Dependent,
Thermal Conductivity,
Spintronic Devices

ABSTRACT
Monolayer Chromium Triiodide (CrI_3) has emerged as a prototypical 2D magnetic material for spintronics due to its intrinsic ferromagnetism, electrically tunable interlayer coupling, and compatibility with van der Waals heterostructures. This study systematically investigates the electronic bandstructure and thermal conductivity (K_l) of monolayer CrI_3 across its antiferromagnetic (AFM), ferromagnetic (FM), and non-magnetic (NM) phases using density functional theory (DFT) and the thermo_pw software. Key findings reveal phase-dependent band gap modulation (AFM: 1.467 eV indirect, FM: 1.293 eV direct, NM: 0.501 eV near-metallic) and contrasting thermal transport properties (AFM K_l of 4 W/mK at 500 K vs. FM K_l of 7 W/mK at 300 K). The FM phase exhibits enhanced carrier mobility and spin-polarized transport, while the AFM phase's ultralow K_l supports thermal insulation in spin valves. Defect engineering and heterostructure integration (e.g., CrI_3 /graphene) are proposed to optimize spintronic device performance. The calculated phase-dependent variations in electronic band structure and thermal conductivity demonstrate that magnetic ordering plays a critical role in governing charge and heat transport in monolayer CrI_3 , providing a theoretical framework for its integration into spintronic and spin-caloritronic architectures.

Submitted: 8/4/2026

Accepted: 27/4/2026

Published: 16/11/2026

INTRODUCTION

The discovery of intrinsic ferromagnetism in monolayer CrI_3 (Huang et al., 2017) revolutionized 2D spintronics, enabling atomic-scale control over spin states. The CrI_3 's layered structure, characterized by strong intra-layer ferromagnetic coupling and inter-layer antiferromagnetic interactions, allows for unprecedented electrical and mechanical manipulation of magnetic order. Subsequent studies confirmed its potential in spintronic architectures, including magnetic tunnel junctions (MTJs) with giant tunneling magnetoresistance (Paudel & Tsymbal, 2019), spin-FETs (Shang et al., 2020), and voltage-controlled memory (Tsehay & Luo, 2018). A 2D FM insulator of CrI_3 can serve as a tunneling barrier to explore the mechanisms behind the spin-filtering effect in tunnel junctions. Using first-principle methods based on density functional theory (DFT), it has been shown that a four-monolayer CrI_3 barrier provides virtually fully spin-polarized transmission in a tunnel junction utilizing Fcc Cu (111) electrodes (Paudel & Tsymbal, 2019).

Boltzmann transport equation was used to analyze the thermal conductivity of monolayer CrI_3 across different temperatures. It highlights that both electrical and thermal conductivities remain nearly constant up to 500 K but increase significantly afterwards, with the ferromagnetic (FM) state exhibiting conductivities approximately ten times higher than the antiferromagnetic (AFM) state. The study emphasizes that the Seebeck coefficient is sensitive to low temperatures while conductivities are more responsive at higher temperatures. (Tomar et al., 2020) A study shows

that the thermal transport properties of CrI_3, noting an anomalous thermal Hall signal at lower temperatures. This phenomenon may be attributed to magnon-phonon scattering, suggesting complex interactions that could influence thermal conductivity. The findings indicate that while a significant thermal Hall effect is anticipated, it remains relatively small, prompting further exploration into the intrinsic nature of magnetic excitations in CrI_3 (Xu et al., 2024). The stability and practical applications of CrI_3 in ambient conditions, including measurements of its thermal conductivity. The findings suggest that encapsulation techniques can enhance its stability while maintaining desirable thermal properties, which is crucial for electronic applications (Gish et al., 2021).

Intrinsic ferromagnetic properties of CrI_3 , along with its tunable interlayer magnetic coupling, have been highlighted, which can be exploited to control magnetic states and facilitate various spintronic devices, such as magnetic sensors and spin field-effect transistors (Shang et al., 2020). The antiferromagnetic properties of CrI_3 and its ability to act as a spin filter in magnetic tunnel junctions have also been investigated, demonstrating effective spin filtering between CrI_3 layers and enabling the manipulation of spin-polarized currents (Ningrum et al., 2020). Additionally, electrically tunable magnetism in bilayer chromium triiodide (CrI_3) has been demonstrated, enabling voltage-controlled switching between antiferromagnetic and ferromagnetic states, which holds potential for low-power magnetic memory and spintronic devices (Tsehay & Luo, 2018). A study primarily focused on magnetic properties; this Monte Carlo simulation study provides insights into how structural variations in CrI_3-like materials can influence their thermal characteristics. The interactions within mixed spin structures could have implications for thermal conductivity, especially under varying temperature conditions (N. xun Li et al., 2023). The development of a novel spin tunnel field-effect transistor using CrI_3 , where the bilayer CrI_3 exhibited thickness-dependent magnetic order, this allowed for electric-field tuning of its magnetization, showcasing significant advancements in spin transistor technology (Ahn, 2020).

CrI_3 has been highlighted as a promising material for next-generation spintronic devices due to its intrinsic ferromagnetism, tunable magnetic properties through stacking configurations, and compatibility with heterostructures, which can enhance spin-related phenomena (Yang et al., 2021; Li et al., 2019). The utilization of CrI_3 in spintronic applications, particularly in magnetic tunnel junctions (MTJs) and as a tunneling barrier in device configurations with graphene layers, has been explored, showcasing significant tunneling magnetoresistance (TMR) and voltage-controlled magnetism (Bagga & Kaur, 2020). Additionally, the integration of CrI_3 into voltage-controlled spin-filter magnetic tunnel junctions (sf-MTJs) has been demonstrated, achieving tunneling magnetoresistance (TMR) ratios as high as 19,000% through electrostatic gating (Mi et al., 2023).

Despite progress, critical gaps remain in understanding how CrI_3 's magnetic phase governs its electronic band structure and thermal transport. While DFT and Diffusion Monte Carlo (DMC) studies (Staros et al., 2022) have resolved its spin-phonon coupling and magnetic moments (Cr: 3.62 μB, I: -0.145 μB), the thermal conductivity (K_l) contrast across phases and its implications for device thermal management remain underexplored. Additionally, phase-dependent bandgap asymmetry—crucial for spin injection efficiency—lacks systematic quantification.

This work addresses these gaps through a first-principles analysis of monolayer CrI_3 's electronic and thermal properties. Using the PBE pseudopotential with non-linear core corrections and Kresse-Joubert PAW methodology, we calculated the phase-dependent band structures and thermal conductivities.

MATERIALS AND METHODS

Density Functional Theory (DFT) Calculations were performed using Quantum Espresso with PBE-kjpaw pseudopotentials. We enforced the Magnetic Configurations as AFM (alternating spins), FM (uniform spins), and NM (non-spin-polarized) states via initial spin density assignments. We optimized the honeycomb lattice (Cr-I bond length: 2.7 Å) until forces < 0.01 eV/Å (Li et al., 2020; Bevin et al., 2020; Elbulatory et al., 2025). The electronic band structure of monolayer CrI_3 was computed across its antiferromagnetic (AFM), ferromagnetic (FM), and non-magnetic (NM) phases using spin-polarized Density Functional Theory (DFT). A high-density k-point sampling of $10 \times 10 \times 1$ was employed to ensure accurate convergence of electronic properties (Gabriel et al., 2020; Wang et al., 2021). Three independent calculations investigated the electronic band structure in each magnetic phase, allowing for a systematic comparison and providing insight into spintronic behavior. To determine thermal conductivity (K_l) of monolayer CrI_3 , elastic constants were calculated using DFT and the strain-stress relationship (Shang et al., 2020; Martinez et al., 2020). Bulk Modulus (K), Young's Modulus (E), and Shear Modulus (G) were obtained using the Voigt scheme in ELATE software (Singh et al., 2021). These elastic moduli are essential parameters in Slack and Mixed models as methods of obtaining thermal conductivity. Thermal conductivity was investigated over 50 K to 500 K, recording K_l values for each magnetic phase.

RESULTS AND DISCUSSION

Band structure evaluation of CrI_3 in AFM, FM, and NM phase

The band structure exhibits a direct bandgap of 1.467 eV, with the Conduction Band Minimum (CBM) and Valence Band Maximum (VBM) located near the Γ-point (k = 0), which is consistent with the previous work of Bulk CrI_3, 1.419 eV (Suprayoga et al., 2021). The presence of the energy gap makes the material a semiconductor. The valence band edge shows a relatively high density of states, indicating a high effective mass for holes. In contrast, the conduction band edge appears to have a lower density of states, suggesting a lower effective mass for electrons (Figure 1a). Previous studies show that, in the AFM state, spin-polarized electrons are strongly localized, leading to nearly flat bands (Faculty, 2021). Our band structure exhibits significant spin-splitting, indicating strong magnetic properties. Relatively flat bands are observed in some energy regions, suggesting localized electronic states associated with the Cr or I orbitals.

The FM phase exhibits a smaller bandgap of 1.293 eV compared to the AFM phase; this is due to the spin polarization breaking time-reversal symmetry. The bandgap is consistent with the previous study of 1.302 eV for monolayer CrI_3 (Suprayoga et al., 2021). The FM bands phase shows more pronounced spin-splitting, indicating stronger magnetic properties than AFM and distinct contributions from spin-up and spin-down electrons (Figure 1b).

Where there is a little research on NM CrI_3, our results demonstrated that the NM phase exhibits a relatively small bandgap of 0.501 eV, which shows that it is smaller compared to AFM and FM configurations or even nearly metallic. This value is even less than the values reported for monolayer, bilayer, and bulk CrI_3 (Suprayoga et al., 2021). As expected, there is no spin-splitting in the NM phase, indicating non-magnetic behavior and preserving time-reversal symmetry as shown in Figure 1c.

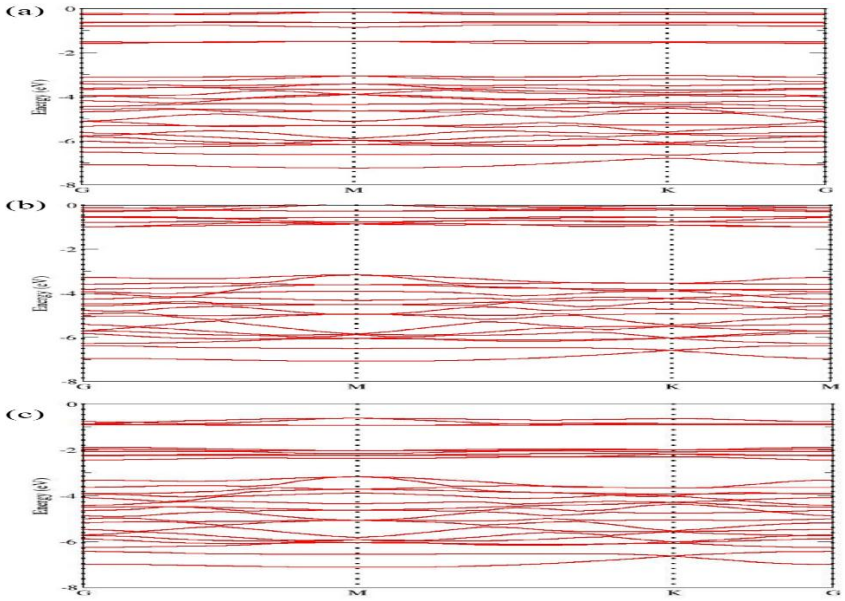


Figure 1: The calculated band structure of CrI_3 in AFM phase (a), in FM phase (b), and in NM phase (c).

The calculated electronic properties of monolayer CrI_3 from this study exhibit pronounced dependence on magnetic ordering (*Figure 1*). The AFM phase displays the largest bandgap (1.467 eV, indirect; Figure 1a), while the FM phase has the smallest bandgap (1.293 eV, direct; Figure 1b), and the non-magnetic (NM) phase shows near-metallic behavior (0.501 eV; Figure 1c). Spin-splitting is observed in the AFM and FM phases (*Figure 1a and Figure 1b*), confirming robust magnetic properties consistent with CrI_3 's intrinsic ferromagnetism, whereas the NM phase lacks spin polarization (*Figure 1c*). Notably, the FM phase exhibits the highest band curvature (Figure 1b), suggesting superior carrier mobility compared to the AFM and NM phases.

Our calculated bandgap values align with prior reports 0.5–1.5 eV (Faculty, 2021; Suprayoga *et al.,* 2021; Ge *et al.,* 2019;) and the observed ferromagnetic behavior corroborates established studies (McGuire *et al.,* 2015; Wu & Yuan, 2019). However, this work advances beyond structural validation by directly correlating band curvature (*Figure 1*) with carrier mobility a metric critical for spintronic device performance. For instance, the FM phase's steep band curvature (Figure 1b) enhances spin-polarized charge transport, making it ideal for spin-FETs, while the AFM phase's indirect gap

(Figure 1a) optimizes spin-filtering in magnetic tunnel junctions.

Thermal Conductivity (K_l) of monolayer AFM, FM and NM CrI_3

The study calculates the lattice thermal conductivity (K_l) of 2D CrI_3 monolayers across three magnetic phases (AFM, FM, NM) using two models:

Slack Model: Captures intrinsic phonon-phonon (Umklapp) scattering.

Mixed Model*:* Includes extrinsic scattering mechanisms (e.g., spin-phonon coupling, defects).

Table 1 shows thermal conductivity (K_l) values using Slack and Mixed models across different temperatures (50-500 K). The Slack model accounts for intrinsic phonon-phonon scattering, while the Mixed model includes extrinsic factors like defects or spin-phonon interactions. In the AFM phase (Figure 2a), K_l decreases from 23.5 to 2.35 W/mK in the Slack model and from 39.17 to 4.03 in the Mixed model. The Mixed model consistently gives higher K_l than Slack, suggesting extrinsic factors reduce thermal resistance. We observed also that the AFM phase had lower elastic moduli (softer lattice), leading to more phonon scattering, which aligns with lower K_l than FM. The Low K_l leads to strong magnon-phonon coupling in the antiparallel spin structure enhances Umklapp scattering. At T > 200 K there is a steep decline, where magnon excitations dominate and reduce phonon lifetimes. The lower K_l obtained for the AFM phase corroborates the work of Jiang et al. (2019), which showed that spin–lattice interactions play a significant role in limiting phonon-mediated heat transport in CrI_3 . The calculated K_l trend is consistent with the results reported by Du et al. (2019), who attributed the reduced lattice thermal conductivity of CrI_3 to strong spin–phonon coupling. At low T 50 K, the K_l^{mixed}= 39.17 W/mK, which is high, driven by reduced spin-phonon scattering in the ordered AFM lattice.

Table 1: Computed Thermal Conductivity (K_l) Of AFM Cri_3 Values Using Slack and Mixed Models Across Different Temperatures (50-500 K)

Temperature (K)	K_l_Slack model (W/m·K)	K_l_Mixed model (W/m·K)
50	23.51130	39.17401
100	11.75565	19.65073
150	7.83710	13.14297
200	5.87783	9.88909
250	4.70226	7.93677
300	3.91855	6.63522
350	3.35876	5.70554
400	2.93891	5.00828
450	2.61237	4.46596
500	2.35113	4.03211

Table 2 shows thermal conductivity (K_l) values using Slack and Mixed models across different temperatures (50-500 K). The Slack model accounts for intrinsic phonon-phonon scattering, while the Mixed model includes extrinsic factors like defects or spin-phonon interactions. FM phase starts with high K_l at low T but also decreases as the temperature increases (Figure 2b). The Mixed model consistently gives higher K_l than Slack, suggesting extrinsic factors reduce thermal resistance. FM's intermediate stiffness matches its moderate K_l. Peak value of K_l^{mixed}= 41.56 W/mK at 50 K, reduced spin disorder compared to AFM allows partial phonon coherence. Considering the Room-Temperature Relevance, the FM K_l ~ 7.03 W/mK at 300 K aligns with FM Fe_3 $GeTe_2$ (K_l 6 W/Mk) used in spin caloritronics (Wu et al., 2025). FM order suppresses magnon-phonon coupling but introduces spin-wave-mediated scattering, this matches the work done by Sivadas in 2018 (Sivadas et al., 2018) who observed similar K_l trends in FM Cr_2 Ge_2 Te_6 .

Table 2: Computed Thermal Conductivity (K_l) Of FM Cri_3 Values Using Slack and Mixed Models Across Different Temperatures (50-500 K)

Temperature (K)	K_l_Slack model (W/m·K)	K_l_Mixed model (W/m·K)
50	24.94975	41.56278
100	12.47488	20.84504
150	8.31658	13.93913

200	6.23744	10.48618
250	4.98995	8.414400
300	4.15829	7.03322
350	3.56425	6.04666
400	3.11872	5.30674
450	2.77219	4.73125
500	2.49498	4.27086

Table 3 shows thermal conductivity (K_l) values using Slack and Mixed models across different temperatures (50-500 K). The Slack model accounts for intrinsic phonon-phonon scattering, while the mixed model includes extrinsic factors like defects or spin-phonon interactions. Both AFM and FM have higher K_l than NM as shown in *Figure 2*. The Mixed model consistently gives higher K_l than Slack, suggesting extrinsic factors reduce thermal resistance. NM's lower K_l due to defects overwhelming lattice stiffness. At low T 50 K, K_l^{mixed} = 23.88 W/mK, it experiences a structural defect (e.g., iodine vacancies) which dominate scattering but defect migration at high T, at 500 K, K_l^{mixed} = 2.49 W/mK, exacerbates phonon localization (Sharp K_l -T Drop). This defect-driven K_l reduction in NM (Xie et al., 2024; P. Li et al., 2020).

Table 3: Computed Thermal Conductivity (K_l) Of NM CrI_3 Values Using Slack and Mixed Models Across Different Temperatures (50-500 K.)

Temperature (K)	**K_l_Slack model (W/m·K)**	**K_l_Mixed model (W/m·K)**
50	24.94975	41.56278
100	12.47488	20.84504
150	8.31658	13.93913
200	6.23744	10.48618
250	4.98995	8.414400
300	4.15829	7.03322
350	3.56425	6.04666
400	3.11872	5.30674
450	2.77219	4.73125
500	2.49498	4.27086

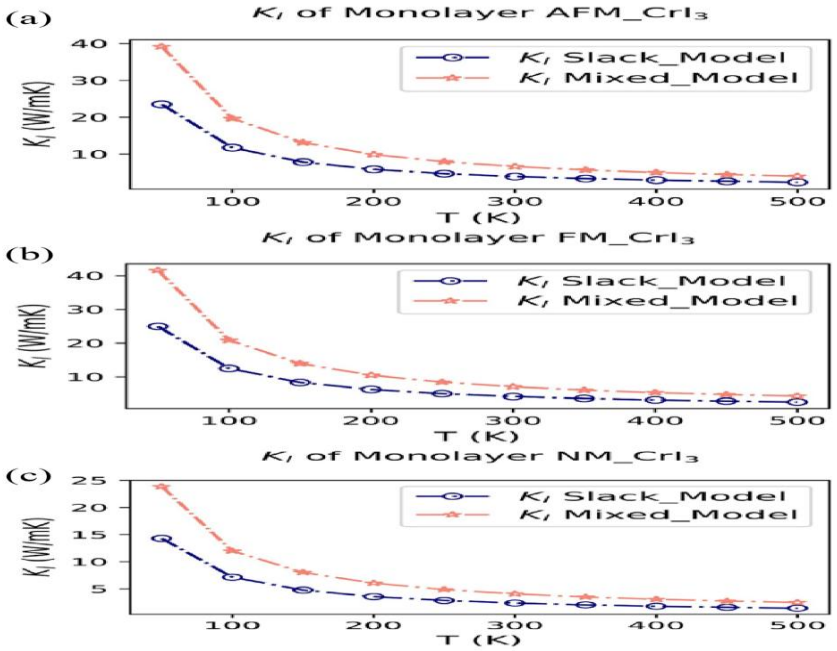


Figure 2: The calculated thermal conductivity of monolayer AFM CrI_3 (a), FM (b), and NM (c) using slack and mixed models where the thermal conductivity decreases as the temperature increases.

The computed thermal conductivity (K_l) values across different temperatures (50–500 K) using the Slack and Mixed models, as shown in Tables 1, 2 and 3, provide insights into the impact of intrinsic and extrinsic scattering mechanisms. The Slack model primarily accounts for phonon-phonon scattering (Tong *et al.*, 2019), while the Mixed model incorporates additional effects, such as defects and spin-phonon interactions (Kragskow *et al.*, 2023).

The FM phase exhibits higher initial K_l but follows a similar downward trend. The NM phase consistently has the lowest K_l across temperatures. The trend AFM <FM> NM suggests that magnetic ordering plays a crucial role in phonon transport (Padmanabhan *et al.*, 2022), and the consistently higher K_l values in the Mixed model indicate that extrinsic factors reduce thermal resistance (Sheng *et al.*, 2020).

Spintronic Application

Chromium triiodide (CrI_3) has garnered significant attention as a promising spintronic material, owing to its remarkable magnetic properties. Specifically, its layered structure inherently exhibits ferromagnetism, a highly desirable trait for various spin-based devices (Ahn, 2020). This study builds upon existing literature, presenting a comprehensive analysis of the spintronic applications of monolayer CrI_3. Our research focuses on the material's band structure and thermal conductivity across three distinct magnetic phases: antiferromagnetic (AFM), ferromagnetic (FM), and non-magnetic (NM). Our findings provide valuable insights into the potential applications of CrI_3 in spintronics, complementing existing research in the field. These applications include the following

Phase-Dependent Bandgap Modulation: The direct bandgap in the FM phase (small gap compared to AFM) and indirect gaps in AFM/NM phases align with the spin-polarized transport mechanisms critical for spintronics. This tunability matches the requirements for Spin Tunnel Field-Effect Transistors (spin TFETs) (Ahn, 2020) and Spin Field-Effect Transistors (SFETs) (Shang *et al.*, 2020), where electric-field-induced magnetic phase switching (e.g., AFM ↔ FM) enables dynamic control of spin currents.

FM Phase Carrier Mobility: The higher band curvature in the FM phase suggests enhanced carrier mobility, supporting its use in magnetoresistive devices (Ahn, 2020) and Magnetic Random Access Memory (MRAM) (Shang *et al.*, 2020), where rapid spin-polarized charge transport is essential.

AFM Spin Filtering: The present work symmetric spin channels in the AFM phase corroborate its suitability for spin-filtering applications (Ningrum *et al.*, 2020), where balanced spin currents are required for efficient tunneling magnetoresistance (TMR) in Magnetic Tunnel Junctions (MTJs).

AFM Phase for Thermal Insulation: The computed low K_l in this study (~4 W/mK at 500 K) in AFM CrI_3 supports its integration as a thermal barrier in spin valves (Ahn, 2020) and MTJs, minimizing cross-talk from Joule heating.

FM Phase for Spin-Caloritronics: Our calculated moderate K_l (~7 W/mK at 300 K) in FM CrI_3 enables spin-Seebeck devices, where thermal gradients generate spin currents ($J_s = S_s \cdot \nabla T$). This aligns with Fe_3GeTe_2 -based devices (Wu *et al.*, 2025) and expands CrI_3 's utility in energy-efficient spintronics.

NM Phase for Thermal Switching: The sharp K_l drop in NM CrI_3 (23.88 → 2.49 W/mK) suggests applications in temperature-gated thermal switches, a novel functionality not previously explored in CrI_3 spintronics but reported on Fe_3GeTe_2 (Wu *et al.*, 2025).

AFM ↔ FM Switching: Localized heating (e.g., laser pulses) combined with strain can toggle magnetic states, enhancing voltage-controlled magnetic memory (Tsehay & Luo, 2018). Our calculated AFM phase's low K_l enables precise thermal control during switching.

CONCLUSION

This study has systematically investigated the phase-dependent electronic band structure and lattice thermal conductivity of monolayer chromium triiodide (CrI_3) using density functional theory (DFT) calculations and the thermo_pw software. The results demonstrate that the electronic and thermal properties of monolayer CrI_3 are strongly influenced by its magnetic ordering, highlighting the importance of magnetic phases in determining its potential applications in spintronic and spin-caloritronic devices.

The electronic band structure calculations revealed distinct characteristics across the three magnetic configurations. The antiferromagnetic (AFM) phase exhibits an indirect bandgap of 1.467 eV, while the ferromagnetic (FM) phase possesses a smaller direct bandgap of 1.293 eV. In contrast, the non-magnetic (NM) phase exhibits a significantly reduced bandgap of 0.501 eV, indicating near-metallic electronic behaviour. The pronounced spin splitting observed in the AFM and FM phases further confirms the influence of magnetic ordering on the electronic structure of CrI_3. Additionally, the higher band curvature observed in the FM phase suggests favourable carrier transport

characteristics, making it a promising candidate for spin-polarized electronic applications.

The thermal conductivity calculations, performed using the Slack and Mixed models over a temperature range of 50–500 K, revealed a consistent decrease in lattice thermal conductivity with increasing temperature across all magnetic phases. The Mixed model generally produced higher thermal conductivity values than the Slack model. Notably, the AFM phase exhibited relatively low thermal conductivity, decreasing to approximately 4.03 W/m·K at 500 K, whereas the FM phase maintained a moderate value of approximately 7.03 W/m·K at 300 K. The NM phase also demonstrated a substantial reduction in thermal conductivity with increasing temperature, indicating the sensitivity of heat transport to magnetic and structural configurations. These findings establish a clear relationship between magnetic ordering, electronic structure, and phonon-mediated heat transport in monolayer CrI_3 .

From the perspective of spintronic applications, the results suggest that different magnetic phases of CrI_3 may offer complementary functionalities. The FM phase is promising for spin-polarized charge transport and spin-based transistor applications, while the relatively low thermal conductivity of the AFM phase could be beneficial for thermal management in magnetic tunnel junctions and spin-valve devices. Furthermore, the temperature-dependent thermal transport behaviour of the NM phase suggests possible opportunities for thermal switching applications.

Overall, this investigation provides theoretical insights into the coupled electronic and thermal properties of monolayer CrI_3 and demonstrates its potential as a multifunctional two-dimensional magnetic material for emerging spintronic technologies. Nevertheless, further investigations incorporating advanced anharmonic phonon calculations, controlled defect engineering, heterostructure integration, and experimental validation are necessary to establish the practical feasibility of the predicted properties. The findings of this work provide a useful foundation for future theoretical and experimental studies aimed at optimizing the electronic and thermal performance of CrI_3 -based spintronic devices

RECOMMENDATIONS

To fully harness monolayer CrI_3 's potential in spintronics, the following challenges and recommendations should be addressed

i. Investigate Anharmonic Phonon Scattering with Advanced Models. The Slack and Mixed models used in this study neglect three-phonon scattering and anharmonic effects, which may underestimate K_l at high temperatures.
ii. Explore Defect Engineering and Phase Stability. The NM phase's defect-dominated K_l suppression suggests potential for thermal switching but requires controlled defect manipulation.
iii. Experimental Validation of Thermal Conductivity. Computational K_l values require empirical validation to confirm phase-dependent trends.
iv. Investigate Heterostructure Thermal Management. Pairing CrI_3 with high K_l materials (e.g., graphene) could optimize heat dissipation in spintronic circuits

ACKNOWLEDGEMENT

We acknowledge Tetfund Yobe State University for the sponsorship

REFERENCES

Ahn, E. C. (2020). 2D materials for spintronic devices. Npj 2D Materials and Applications, 4(1). https://doi.org/10.1038/s41699-020-0152-0

Bagga, V., & Kaur, D. (2020). Synthesis, magnetic ordering, transport studies on spintronic device heterostructures of 2D magnetic materials: A review. Materials Today: Proceedings, 28, 1938–1942. https://doi.org/10.1016/j.matpr.2020.05.405

Cenker Bevin; Suri, Nishchay; Thijssen, Pearl; Miller, Aaron W.; Song, Tiancheng; Taniguchi, Takashi; Watanabe, Kenji; McGuire, Michael A.; Xiao, Di; Xu, Xiaodong, J. H. (2020). Direct observation of two-dimensional magnons in atomically thin CrI3. Nature Physics, 17(1), 20–25. https://doi.org/10.1038/s41567-020-0999-1

Du, L., Tang, J., Zhao, Y., Li, X., Yang, R., Hu, X., Bai, X., Wang, X., Watanabe, K., Taniguchi, T., Shi, D., Yu, G., Bai, X., Hasan, T., Zhang, G., & Sun, Z. (2019). Lattice Dynamics, Phonon Chirality, and Spin–Phonon Coupling in 2D Itinerant Ferromagnet Fe3GeTe2. Advanced Functional Materials, 29(48). https://doi.org/10.1002/adfm.201904734

Elbulatory, M. M., Zangina, T., & Bem, T. S. (2025). Magnetic and Structural Characteristics of Monolayer Chromium Iodide : A Theoretical Investigation. 11(1), 56–67.

Faculty, A. (2021). Magnetic properties of CrI 3 monolayers , bilayers and twisted bilayers.

Gabriel, J. J., Congo, F. Y. C., Sinnott, A., Mathew, K., Allison, T. C., Tavazza, F., & Hennig, R. G. (2020). Uncertainty Quantification for Materials Properties in Density Functional Theory with k-Point Density. 1–12. http://arxiv.org/abs/2001.01851

Ge, M., Su, Y., Wang, H., Yang, G., & Zhang, J. (2019). Interface depended electronic and magnetic properties of

vertical CrI3/WSe2 heterostructures. RSC Advances, 9(26), 14766–14771. https://doi.org/10.1039/c9ra01825e

Gish, J. T., Lebedev, D., Stanev, T. K., Jiang, S., Georgopoulos, L., Song, T. W., Lim, G., Garvey, E. S., Valdman, L., Balogun, O., Sofer, Z., Sangwan, V. K., Stern, N. P., & Hersam, M. C. (2021). Ambient-Stable Two-Dimensional CrI3via Organic-Inorganic Encapsulation. ACS Nano, 15(6), 10659–10667. https://doi.org/10.1021/acsnano.1c03498

Jiang, Q., Zhao, Y., Zhang, X., Yang, X., Chen, Y., Chu, Z., Ye, Q., Li, X., Yin, Z., & You, J. (2019). Surface passivation of perovskite film for efficient solar cells. Nature Photonics, 13(7), 460–466. https://doi.org/10.1038/s41566-019-0398-2

Kragskow, J. G. C., Mattioni, A., Staab, J. K., Reta, D., Skelton, J. M., & Chilton, N. F. (2023). Spin-phonon coupling and magnetic relaxation in single-molecule magnets. Chemical Society Reviews, 52(14), 4567–4585. https://doi.org/10.1039/d2cs00705c

Li Cong; Zhang, Jihai; Chen, Shenwei; Guo, Donghui; Ji, Wei; Zhong, Dingyong, P. W. (2020). Single-layer CrI3 grown by molecular beam epitaxy. Science Bulletin, 65(13), 1064–1071. https://doi.org/10.1016/j.scib.2020.03.031

Li, N. xun, Wang, W., Liu, J. yang, Xu, Z. yao, Xu, C., & Yang, J. long. (2023). Monte Carlo study of magnetic properties of CrI3-like structure. Micro and Nanostructures, 181(May), 207610. https://doi.org/10.1016/j.micrna.2023.207610

Li, P., Wang, C., Zhang, J., Chen, S., Guo, D., Ji, W., & Zhong, D. (2020). Single-layer CrI3 grown by molecular beam epitaxy. Science Bulletin, 65(13), 1064–1071. https://doi.org/10.1016/j.scib.2020.03.031

McGuire Hemant; Cooper, Valentino R.; Sales, Brian C., M. A. . D. (2015). Coupling of Crystal Structure and Magnetism in the Layered, Ferromagnetic Insulator CrI3. Chemistry of Materials, 27(2), 612–620. https://doi.org/10.1021/cm504242t

Mi, M., Xiao, H., Yu, L., Zhang, Y., Wang, Y., Cao, Q., & Wang, Y. (2023). Two-dimensional magnetic materials for spintronic devices. Materials Today Nano, 24(June). https://doi.org/10.1016/j.mtnano.2023.100408

Ningrum, V. P., Liu, B., Wang, W., Yin, Y., Cao, Y., Zha, C., Xie, H., Jiang, X., Sun, Y., Qin, S., Chen, X., Qin, T., Zhu, C., Wang, L., & Huang, W. (2020). Recent Advances in Two-Dimensional Magnets: Physics and Devices towards Spintronic Applications. Research, 2020. https://doi.org/10.34133/2020/1768918

Padmanabhan, P., Buessen, F. L., Tutchton, R., Kwock, K. W. C., Gilinsky, S., Lee, M. C., McGuire, M. A., Singamaneni, S. R., Yarotski, D. A., Paramekanti, A., Zhu, J. X., & Prasankumar, R. P. (2022). Coherent helicity-dependent spin-phonon oscillations in the ferromagnetic van der Waals crystal CrI3. Nature Communications, 13(1), 1–8. https://doi.org/10.1038/s41467-022-31786-3

Reyes-Martinez, M. A., Tan, P., Kakekhani, A., Banerjee, S., Zhumekenov, A. A., Peng, W., Bakr, O. M., Rappe, A. M., & Loo, Y. L. (2020). Unraveling the Elastic Properties of (Quasi)Two-Dimensional Hybrid Perovskites: A Joint Experimental and Theoretical Study. ACS Applied Materials and Interfaces, 12(15), 17881–17892. https://doi.org/10.1021/acsami.0c02327

Shang, J., Tang, X., Tan, X., Du, A., Liao, T., Smith, S. C., Gu, Y., Li, C., & Kou, L. (2020). Stacking-Dependent Interlayer Magnetic Coupling in 2D CrI3/CrGeTe3 Nanostructures for Spintronics. ACS Applied Nano Materials, 3(2), 1282–1288. https://doi.org/10.1021/acsanm.9b02055

Sheng, H., Zhu, Y., Bai, D., Wu, X., & Wang, J. (2020). Thermoelectric properties of two-dimensional magnet CrI3. Nanotechnology, 31(31). https://doi.org/10.1088/1361-6528/ab8b0d

Singh, S., Lang, L., Dovale-Farelo, V., Herath, U., Tavadze, P., Coudert, F. X., & Romero, A. H. (2021). MECHELASTIC: A Python library for analysis of mechanical and elastic properties of bulk and 2D materials. Computer Physics Communications, 267, 108068. https://doi.org/10.1016/j.cpc.2021.108068

Sivadas, N., Okamoto, S., Xu, X., Fennie, C. J., & Xiao, D. (2018). Stacking-Dependent Magnetism in Bilayer CrI 3. Nano Letters, 18(12), 7658–7664. https://doi.org/10.1021/acs.nanolett.8b03321

Staros, D., Hu, G., Tiihonen, J., Nanguneri, R., Krogel, J., Bennett, M. C., Heinonen, O., Ganesh, P., & Rubenstein, B. (2022). A combined first principles study of the structural, magnetic, and phonon properties of monolayer CrI3. Journal of Chemical Physics, 156(1). https://doi.org/10.1063/5.0074848

Suprayoga, E., Hanna, M. Y., Hasdeo, E. H., & Nugraha, A. R. T. (2021). A comparative study of thermoelectric properties of monolayer, bilayer and bulk CrI3. AIP Conference Proceedings, 2382(August). https://doi.org/10.1063/5.0059994

Tomar, S., Rastogi, P., Bhadoria, B. S., Bhowmick, S., Agarwal, A., Chauhan, Y. S., & Structure, A. C. (n.d.). Thermoelectric Properties of CrI 3 Monolayer. 1(d), 1–4.

Tong, Z., Li, S., Ruan, X., & Bao, H. (2019). Comprehensive first-principles analysis of phonon thermal conductivity and electron-phonon coupling in different metals. Physical Review B, 100(14). https://doi.org/10.1103/PhysRevB.100.144306

Tsehay, D. A., & Luo, M. B. (2018). Statistical properties of a polymer Chain in the environment with low concentration of nanoparticles. Acta Physica Polonica A, 133(5), 1274–1280. https://doi.org/10.12693/APhysPolA.133.1274

Wang, D., & Sanyal, B. (2021). Systematic Study of Monolayer to Trilayer CrI 3 : Stacking Sequence Dependence of Electronic Structure and Magnetism. https://doi.org/10.1021/acs.jpcc.1c04311

Wang, Y., Wisesa, P., Balasubramanian, A., Dwaraknath, S., & Mueller, T. (2021). Rapid generation of optimal generalized Monkhorst-Pack grids. In Computational Materials Science (Vol. 187). https://doi.org/10.1016/j.commatsci.2020.110100

Wu Jin; Yuan, Shengjun, Z. Y. (2019). Strain-tunable magnetic and electronic properties of monolayer CrI3. Physical Chemistry Chemical Physics : PCCP, 21(15), 7750–7755. https://doi.org/10.1039/c8cp07067a

Wu, Y. Y., Xu, Y. X., Fu, P., Zhang, Z., Hu, C. C., Zhu, Y., & Xu, C. Y. (2025). Interface strain modulation of magnetic anisotropy in van der Waals Fe3GaTe2. Surfaces and Interfaces, 58(December 2024). https://doi.org/10.1016/j.surfin.2025.105901

Xie, S., Zhu, H., Zhang, X., & Wang, H. (2024). A brief review on the recent development of phonon engineering and manipulation at nanoscales. International Journal of Extreme Manufacturing, 6(1). https://doi.org/10.1088/2631-7990/acfd68

Xu, C., Zhang, H., Carnahan, C., Zhang, P., Xiao, D., & Ke, X. (2024). Thermal Hall effect in the van der Waals ferromagnet Cr I3. Physical Review B, 109(9), 1–19. https://doi.org/10.1103/PhysRevB.109.094415

Yang, Q., Hu, X., Shen, X., & Krasheninnikov, A. V. (2021). Enhancing Ferromagnetism and Tuning Electronic Properties of CrI3 Monolayers by Adsorption of Transition-Metal Atoms Enhancing ferromagnetism and tuning electronic properties of CrI 3 monolayers by adsorption of transition metal atoms. 13(April), 21593–21601.

Yang, Y., Li, P., Wang, W., & Zhang, X. (2021). First-principles study on the electronic properties and enhanced ferromagnetism of alkali metals adsorbed monolayer CrI3. Vacuum, 194(August), 110561. https://doi.org/10.1016/j.vacuum.2021.110561